Design, Synthesis, and Biological Evaluation of Semicarbazide-Sensitive Amine Oxidase (SSAO) Inhibitors with Anti-inflammatory Activity

Eric Y. Wang,* Hongfeng Gao, Luisa Salter-Cid, Jun Zhang, Li Huang, Erika M. Podar, Andrew Miller, Jingjing Zhao, Anne O'Rourke, and Matthew D. Linnik

La Jolla Pharmaceutical Company, 6455 Nancy Ridge Drive, San Diego, California 92121

Received June 7, 2005

In an attempt to examine the effect of inhibition of semicarbazide-sensitive amine oxidase (SSAO; EC 1.4.3.6, also known as VAP-1) as a novel anti-inflammatory target, the structure/mechanism based design and synthesis of a series of novel hydrazino-containing small molecules are described. The in vitro biological results show that compounds **4a**,**c** are highly potent SSAO inhibitors with notable selectivity toward SSAO over monoamine oxidases A and B (MAO-A and MAO-B). SAR studies based on compound **4c** were performed, and the results are discussed. The most potent and selective compound, **4a** (IC_{50} = 2 nM), is an orally active, competitive, and apparently irreversible inhibitor of SSAO that is effective at reducing disease incidence and severity in an in vivo animal disease model of multiple sclerosis.

Introduction

Semicarbazide-sensitive amine oxidase (SSAO) is a common name for a group of enzymes, containing copper and quinone cofactor[1] and sensitive to semicarbazide, that converts primary amines into the corresponding aldehydes, while releasing ammonia and hydrogen peroxide:[2]

$$RCH_2NH_2 + H_2O + O_2 \xrightarrow{SSAO} RCHO + H_2O_2 + NH_3$$

SSAO is found in a great variety of species from prokaryotes to eukaryotes. In mammals, two forms of the SSAO protein have been identified: a tissue-bound form and a soluble plasma form.[3] The tissue-bound SSAO contains a short intracellular domain, a single transmembrane domain, and a long extracellular domain that contains the active site.[4] Plasma SSAO appears to be the result of proteolytic cleavage of membrane-bound SSAO.

Cloning of the adhesion molecule vascular adhesion protein-1 (VAP-1) revealed that it is identical to membrane-bound SSAO.[5] In humans, cell-associated SSAO is widely expressed in endothelial, smooth muscle, and adipose cells.[6] Cell-surface expression of SSAO is tightly regulated and is significantly upregulated at sites of inflammation.[6a,7] SSAO is unique among other endothelial cell-expressed adhesion molecules because of its amine oxidase enzymatic activity. Studies have shown that SSAO-mediated adhesion and transendothelial migration of leukocytes through endothelial cell layers is mediated by its enzymatic activity and can be blocked by small-molecule inhibitors.[8] It has been reported that increases in the levels of plasma and/or membrane-associated SSAO occur in many inflammation-associated diseases, including rheumatoid arthritis, inflammatory bowel disease, type 1 and type 2 diabetes, atherosclerosis, and chronic heart failure.[9] The possible involvement of SSAO in the inflammatory processes associated with Alzheimer's disease has also been reported.[10]

Recent results with transgenic mice overexpressing human SSAO support these disease associations.[11,12] SSAO-deficient mice are symptom-free in the resting state but display impaired leukocyte adhesion to endothelial cells of inflamed vessels,[12] further supporting a role for this enzyme in inflammation. The fact that SSAO has both enzymatic and adhesion activities combined with the strong correlation between its upregulation in many inflammatory conditions makes it an interesting therapeutic target for drug discovery.

Several series of compounds have been reported in the literature as SSAO inhibitors (Chart 1). The majority of reported SSAO inhibitors were either originally developed for other therapeutic uses or are simple chemical reagents with highly reactive structural element(s).[13] Most of these compounds lack the combination of high potency and selectivity for SSAO. For example, phenelzine is equally potent on SSAO and MAO-A.[14] MDL 72161, a fluoroallylamine derivative that was originally designed as MAO-B inhibitor for the treatment of Parkinson's disease, exhibits high inhibitory potency on rat aorta SSAO (IC_{50} = 2.5 nM) with no apparent selectivity over MAOs.[15] On the other hand, MDL 72274, a chloroallylamine derivative, was reported to be a potent and selective rat aorta SSAO (IC_{50} = 8 nM) inhibitor.[15]

As part of a continuing effort to explore novel approaches for treating acute and chronic inflammatory diseases, we became interested in examining SSAO as a therapeutic target. We herein report the structure/mechanism based inhibitor design and synthesis of a series of hydrazino-containing small-molecule inhibitors of SSAO. The synthesized compounds were evaluated in an in vitro inhibition assay against SSAO in rat lung homogenates. Structure−activity relationship (SAR) studies based on compound **4c** were conducted, and the results are discussed. Enzyme kinetic and pharmacokinetic studies were also performed for the most potent compound **4a**. In addition, compound **4a** was further evaluated in an in vivo animal disease model of human multiple sclerosis. In vivo SSAO inhibition with compound **4a** produced a reduction in disease incidence and severity in a murine model of acute experimental autoimmune encephalomyelitis. These results suggest that SSAO inhibition may represent a novel approach for the treatment of inflammatory diseases.

Chemistry

The general synthetic routes for the preparation of compounds **4**, **7**, **9**, and **11** are depicted in Scheme 1.

* To whom correspondence should be addressed. Phone: (858) 646-6616. Fax: (858) 626-2845. E-mail: eric.wang@ljpc.com.

10.1021/jm050538l CCC: $33.50
Published on Web 03/14/2006

Chart 1. Some Known SSAO Inhibitors

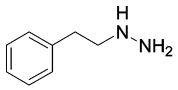

Phenelzine

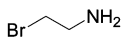

2-bromoethylamine

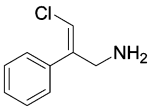

MDL 72274

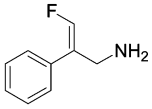

MDL 72161

Compounds **2** were prepared from commercially available compounds **1** according to the literature procedures.[16] The alkylations of compounds **2** with *tert*-butyl carbazate or di-*tert*-butylhydrazodiformate were conducted in the presence of Et_3N or NaH, respectively, which provided compounds **3** and **5**. Compounds **4** were obtained as hydrochloride salts in good yields upon removing the Boc group from compounds **3** under acidic conditions. Further SAR studies were performed on the basis of compound **4c**. Thus, compounds **6** were prepared by alkylation of compound **5c** with a variety of alkyl halides in the presence of NaH. Compounds **7** were then obtained as hydrochloride salts by removing the Boc protecting groups from compounds **6** under acidic conditions. Compounds **8** were made by alkylation of compound **3c** with a variety of alkyl halides in the presence of diisopropylethylamine. Upon stirring compounds **8** under acidic conditions, compounds **9** were obtained as hydrochloride salts. Compound **11** was obtained from the deprotection of compound **10** that was prepared by dimethylation of compound **3b**.

In an attempt to examine the effect of vinylic fluorine substitution on SSAO potency, we synthesized compound **15** as shown in Scheme 2. Thus, compound **14** was obtained through a coupling reaction of compound **12** and compound **13**, which were prepared according to literature procedures.[17] Upon two consecutive deprotections, compound **15** was obtained as the hydrochloride salt.

Results and Discussion

The inhibitory properties of all desired final compounds toward SSAO were initially evaluated in vitro with a radiochemical assay[18] using benzylamine-^{14}C as substrate. A crude rat lung homogenate was used as the source of SSAO for the routine potency measurements.[19] The inhibitory properties of compounds that showed potent SSAO inhibition (IC_{50} < 100 nM) were further evaluated against recombinant human MAO-A and MAO-B in vitro with a coupled colorimetric assay.[20] The ratios of IC_{50} values for SSAO inhibition and MAO inhibition were taken as an approximate index of selectivity for the tested compounds. Table 1 summarizes the in vitro biological results for the synthesized compounds. The approximate IC_{50} values, presented in Table 1, were calculated using GraphPad Prism software from the inhibition curves obtained with an inhibitor concentration between 10^{-3} and 10^{-10} M.

The in vitro data show that compounds **4a**−**d** are highly potent and selective SSAO inhibitors. Comparing these four compounds on the basis of the substitution on the phenyl ring, the order of potency is H > 4-Cl > 2-Me > 4-F, while the order of selectivity is H > 4-F > 2-Me > 4-Cl. The result indicates that the ring substitution has limited effect on potency while having dramatic impact on selectivity. The aqueous solubility tests show that compounds **4a**,**c** are highly soluble at pH 7.4 while compounds **4b**,**d** are less soluble. The vinylic fluorine substitution, compound **15**, also provides potent SSAO inhibition with less specificity toward SSAO.

SAR studies on additional alkyl groups attached to either of the hydrazine nitrogen atoms were performed on the basis of compound **4c**. The in vitro results, as shown in Table 1, reveal that the introduction of an additional alkyl group attached to either of the hydrazine nitrogen atoms results in progressively lower potency compared with the parent compound **4c**. The potency of compounds decreases as the size of alkyl group attached to either of the hydrazine nitrogen atoms increases. The compounds lose potency completely when a bulky alkyl group (i.e. benzyl group) is attached to either hydrazine nitrogen atom. Moreover, the terminal nitrogen atom is more sensitive to the reduction of potency when an additional alkyl group is attached, which can be attributed to the increased size of the molecule that makes it unable to bind to TPQ.

Experiments were performed to determine the kinetic characteristics of the inhibition of SSAO produced by compound **4a**. Analysis of kinetic data reveals that the kinetics is consistent with a first-order inhibition process. The apparent K_m increased, while V_{max} stays unchanged as the concentration of compound **4a** increases.[21] These data demonstrate that compound **4a** is a competitive inhibitor of SSAO and suggest that compound **4a** occupies the substrate-binding pocket of SSAO.

Dialysis experiments were performed using enzyme plus inhibitor to determine whether **4a** is a reversible or irreversible SSAO inhibitor. The results revealed that enzyme inhibition induced by **4a** is minimally modified by 24 h dialysis at 4 °C, indicating that compound **4a** acts as an apparent irreversible inhibitor of SSAO.[21] Compound **4a** was further assessed as a time-dependent inhibitor of SSAO by using the method described by Kitz and Wilson.[22] Increasing concentration of **4a** or the duration of preincubation time with **4a** resulted in greater enzyme inhibition (Figure 1). These results indicated that compound **4a** is a time-dependent inhibitor of SSAO.

The in vivo pharmacokinetic (PK) profile of compound **4a** was established in rats after per os (po) administration of 5.0 mg/kg. As shown in Figure 2, a single oral dose of compound **4a** was administered to female Sprague Dawley rats.[23] The PK parameters of compound **4a** are summarized in Table 2. The results indicate that compound **4a** is rapidly absorbed after oral administration as indicated by short T_{max} with a mean C_{max} value of 366 ng/mL. Compound **4a** has oral bioavailability and a relatively long elimination half-life in rat plasma, presumably due to high plasma protein binding, as has been shown in ADMET studies of compound **4a**.[21]

Inhibition of SSAO with compound **4a** has shown in vivo efficacy in several animal disease models.[24] To further examine the effect of SSAO inhibition on a chronic neurological inflammatory disease, we tested compound **4a** in an animal model of human multiple sclerosis. Multiple sclerosis is a chronic immune-mediated disease of the CNS characterized by patchy perivenular inflammatory infiltrates in areas of demyelination and axonal loss. Experimental autoimmune encephalitis (EAE) in rodents is a well-characterized and reproducible animal model of human multiple sclerosis.[25] In general, EAE animal models can be induced in mice by immunization with encephalitogenic myelin antigens in the presence of adjuvant. The pathogenesis of EAE comprises presentation of myelin antigens to T cells in the periphery, migration of activated T cells to the

Scheme 1[a]

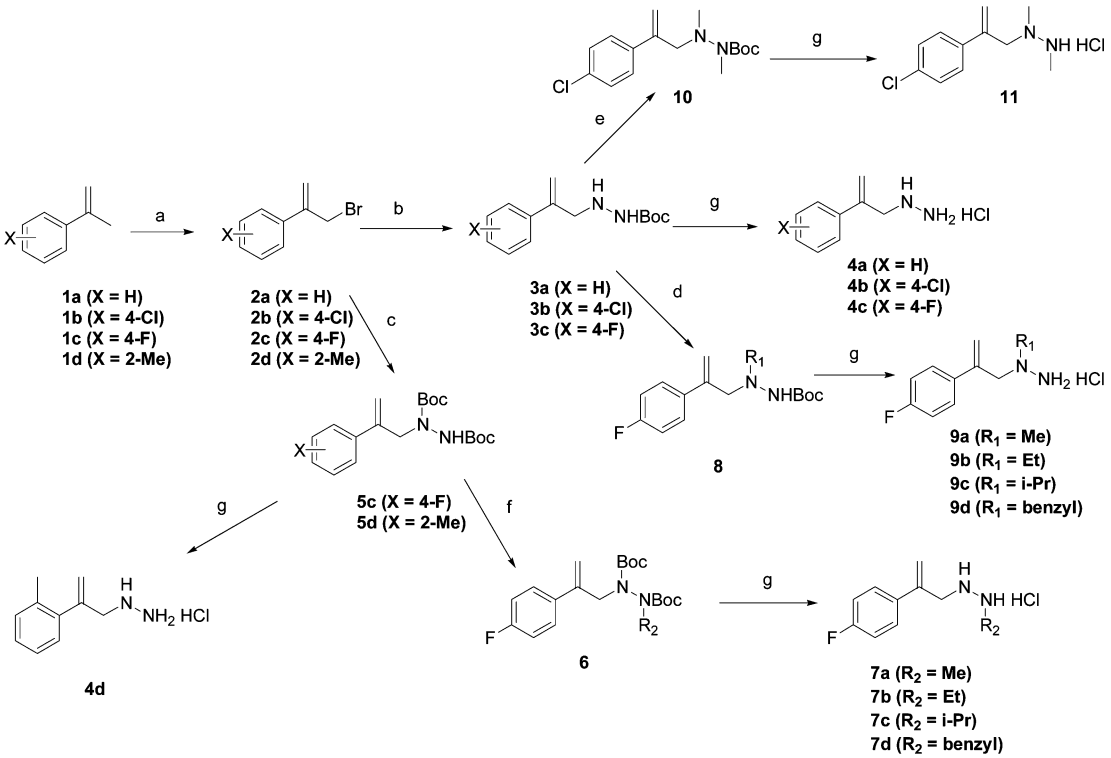

[a] Conditions. (a) Method A: NBS, CCl_4, reflux (for the preparation of **2a**−**c**), Method B: $Yb(OTf)_3$−TMSCl, NBS, CH_2Cl_2−THF (4:1), rt (for the preparation of **2d**). (b) $H_2NNHBoc$, NEt_3, MeOH, reflux. (c) BocNHNHBoc, NaH, DMF, rt. (d) RX (X = I or Br), DIEA, DMF, rt. (e) MeI, NaH, DMF, rt. (f) RX (X = I or Br), NaH, DMF, rt. (g) HCl, Et_2O, MeOH, rt.

Scheme 2[a]

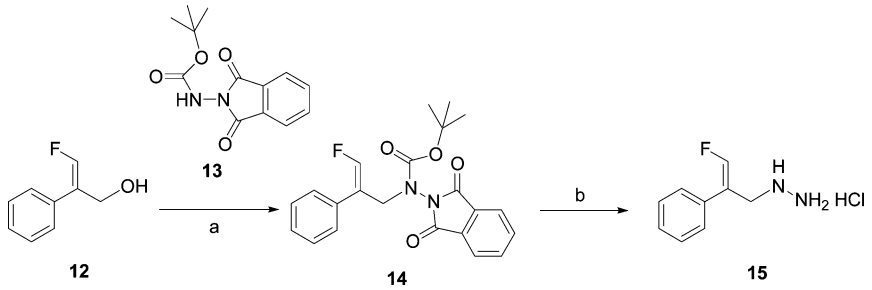

[a] Conditions. (a) PPh_3, DEAD, THF, rt. (b) (i) NH_2NHMe, THF, rt; (ii) MeOH, 4.0 M HCl in 1,4-dioxane, rt.

CNS, and development of inflammation and demyelination upon recognition of the same antigens in the CNS.

As shown in Figure 3, the vehicle-treated group showed an 80% disease incidence and moderate clinical severity during the study period. In contrast, compound **4a**-treated mice exhibited a statistically significant reduction of disease severity relative to vehicle, with 50% of mice affected. Statistically significant differences in disease severity between the **4a** and vehicle-treated groups continued after stopping compound **4a** administration and were observed until the end of the study (day 30). In addition, there is no statistically significant difference in disease severity between **4a** and the positive control group ($p = 0.18$).

Compound **4a** treatment also prevented body weight loss in the mice during the dosing period relative to vehicle-treated animals ($p = 0.04$). As expected, the loss of body weight correlated with the clinical severity in vehicle-treated mice. In addition, the inhibitory effect of compound **4a** on the acute EAE development persisted for 1 week after the last treatment (day 25).

Table 1. Inhibitory Potencies at SSAO, MAO-A, and MAO-B

compd	SSAO IC_{50}[a] (nM)	MAO-A IC_{50} (nM)	MAO-B IC_{50} (nM)
4a	2.0 ± 0.21	1300 ± 180	71000 ± 5200
4b	3.0 ± 0.15	1000 ± 160	24500 ± 2300
4c	6.1 ± 0.51	6000 ± 250	81000 ± 3600
4d	4.0 ± 0.26	2000 ± 150	90000 ± 8900
15	5.0 ± 0.32	2800 ± 400	650 ± 100
7a	1.7 ± 0.12	ND[b]	ND
7b	2.3 ± 0.25	ND	ND
7c	>1000	ND	ND
7d	>1000	ND	ND
9a	240 ± 40	ND	ND
9b	630 ± 55	ND	ND
9c	420 ± 30	ND	ND
9d	>1000	ND	ND
11	2700 ± 360	ND	ND

[a] The values of IC_{50} (μM) are the means obtained from five concentrations of each inhibitor studied at a substrate (benzylamine-^{14}C) concentration of 20 mM, while MAO-A and MAO-B activities were blocked with clorgyline and pargyline at 1.0 μM, respectively. [b] ND = not determined.

It is well-recognized that certain hydrazine-containing compounds are capable of inducing organ damage, including liver

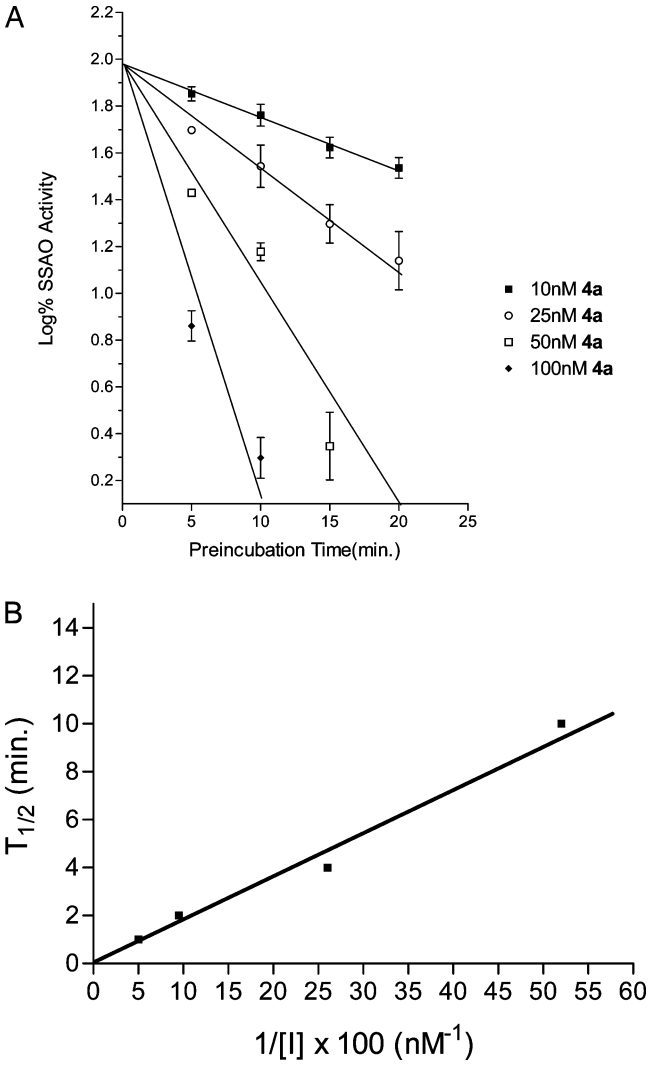

Figure 1. (A) Preincubation time-dependent inhibition of rat lung SSAO by 10 nM (■), 25 nM (○), 50 nM (□), and 100 nM (◆) **4a**. Each point is the mean of duplicate determinations expressed as a percentage of corresponding control samples preincubated without inhibitor. (B) Kitz and Wilson replot of the data.

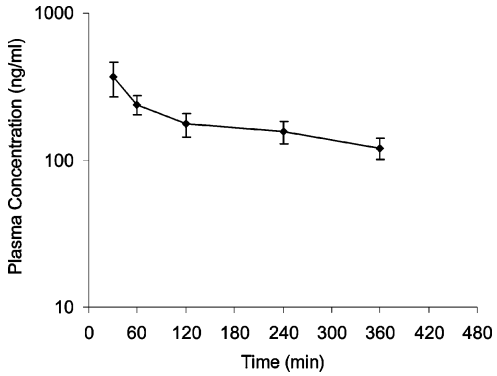

Figure 2. Plasma concentration profile of **4a** in cannulated rats, po 5.0 mg/kg.

damage. The possibility therefore exists that part or all of the benefit attributed to compound **4a** in the acute EAE model could be due to corticosteroid induction secondary to liver toxicity, rather than the effect of SSAO inhibition. Corticosteroids were not measured in this experiment, which can be seen as a limitation of the experiment. However, there is good reason to believe that the effect of **4a** in the acute EAE model is in part due to SSAO inhibition. The beneficial effect of inhibiting of

Table 2. Plasma Pharmacokinetic Profile of **4a**[a]

Dose (mg/kg), po	5	$T_{1/2}$ (min)	677 ± 99
T_{max} (min)	30 ± 0	AUC_{all} (min × ng/mL)	80 415 ± 17 815
C_{max} (ng/mL)	366 ± 116	AUC_{INF} (min × ng/mL)	19 8447 ± 40 977

[a] Mean ± SD (n = 3). Pharmacokinetic parameters were derived from noncompartmental model using WinNonlin 4.0.1.

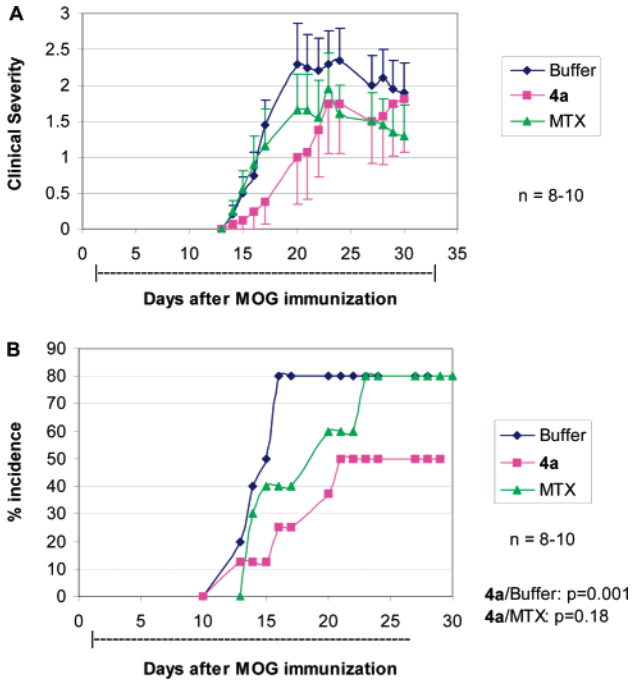

Figure 3. (A) Compound **4a** reduces clinical severity of acute EAE in mice. (B) Compound **4a** reduces the disease incidence of acute EAE in mice. Groups of 8−10 mice received either **4a** at 20 (mg/kg)/dose or vehicle control, daily for 25 consecutive days while methotrexate (MTX) in saline (3 mg/kg, 3× per week) was used as positive control. Dosing was initiated 1 day after the immunization, and all doses were administered ip. Animals were monitored for disease incidence and clinical severity based on signs of neurological impairment, paralysis, and death according to a prospectively defined scoring system based on a 0−5 scale, where 0 indicates normal locomotion and motor function and 5 indicates death.

SSAO in adhesion, acute, and chronic inflammation has been demonstrated by a variety of interventions, including antibodies, enzyme inhibitors, gene knockout, and topaquinone mutant.[12,13,24,26] The inhibitory antibodies and genetic mutants were not reported to be hepatotoxic, and the acute antiinflammatory effects are observed within the first few hours of administration. These well-controlled studies provide strong support for the hypothesis that SSAO inhibition reduces leukocyte trafficking at sites of inflammation, with a resultant reduction in local inflammation. They are also consistent with the hypothesis that the benefit observed with **4a** in the acute EAE model is in part due to SSAO inhibition.

Comparable results on the effects of percentage disease incidence and clinical severity were also observed when MDL 72974a, a known potent SSAO inhibitor, was used in a separate acute EAE study.[21]

Conclusion

A series of hydrazino-containing compounds have been synthesized and evaluated as SSAO inhibitors. Compounds **4a**,**4c** are highly potent and selective SSAO inhibitors. The SAR studies based on **4c** show that potency decreases when an additional alkyl group is attached to either hydrazine nitrogen atom. The compounds lose potency completely when an

additional larger alkyl group (i.e., benzyl group) is attached to either hydrazine nitrogen atom. Terminal hydrazine nitrogen atom is more sensitive to the reduction of potency when an additional alkyl group is attached. Substitution on the phenyl ring did not change compound potency significantly but had a profound effect on the selectivity of the compounds. In addition, the vinylic fluorine substitution, compound **15**, has less influence on potency but has significant effect on selectivity. The most potent and selective compound, **4a**, is an orally active, competitive, and apparently irreversible inhibitor of SSAO. Inhibition of SSAO with compound **4a** in vivo produced a reduction in disease incidence and severity in a murine model of human multiple sclerosis. These results suggest that inhibition of SSAO may be an effective approach for inhibiting inflammation.

The biological results obtained with compound **4a** in an in vivo model of multiple sclerosis illustrate the potential utility of inhibiting SSAO activity in a chronic inflammatory disease.[24] While the hydrazine moiety may limit the clinical utility of **4a** for interventions requiring chronic administration, the SAR information gained from this series may be relevant to the design of small-molecule SSAO inhibitors in related series.

Experimental Section

Melting points were recorded on a Thomas-Hoover capillary melting point apparatus and are uncorrected. Elemental analyses were performed by NuMega Resonance Labs, San Diego, CA. ^{1}H NMR spectra were recorded on Bruker NMR spectrometers operating at 300.1 and at 500 MHz. MS spectra (ESI) were performed on a LCQ Finnigan mass spectrometer in positive mode. High-resolution mass spectra (HRMS) were recorded on IonSpec Ultima FTMS instrument at the Scripps Center for Mass Spectrometer in The Scripps Research Institute, La Jolla, CA. Analytical chromatography was performed on Whatman PE Sil G/UV silica gel plate (250 μM). Flash column chromatography was performed using J. T. Baker silica gel (40 μM). All commercially obtained reagents were used as received unless otherwise noted.

General Procedure for the Preparation of Compounds 3. A mixture of $H_2NNHBoc$ (2.0 equiv) and NEt_3 (2.0 equiv) in MeOH (30 mL) was stirred at room temperature for 20 min. To this stirred solution was added α-bromomethylstyrene[16a] (1.0 equiv). The resulting mixture was kept at gentle reflux and monitored with thin-layer chromatography (TLC). After refluxing for 3 h, the TLC showed that the reaction was completed. The reaction mixture was concentrated in vacuo. The residue was purified by flash column chromatography (silica gel, 10% EtOAc/hexane) to give the desired product.

(a) *N*-*tert*-Butoxycarbonyl-*N*′-(2-phenylallyl)hydrazine (3a). The title compound was obtained as a white solid (1.34 g, 44%). mp: 79−80 °C. ^{1}H NMR ($CDCl_3$, 300 MHz): δ 1.50 (s, 9H), 3.90 (s, 2H), 5.30 (s, 1H), 5.51 (s, 1H), 7.26−7.38 (m, 3H), 7.45−7.52 (m, 2H). ESMS: *m*/*z* 271.1 $(M + Na)^+$.

(b) *N*-*tert*-Butoxycarbonyl-*N*′-[2-(4-chlorophenyl)allyl]hydrazine (3b). The title compound was obtained as a white solid (2.7 g, 32%). mp: 94−96 °C. ^{1}H NMR ($CDCl_3$, 300 MHz): δ 1.45 (s, 9H), 3.85 (s, 2H), 5.27 (s, 1H), 5.45 (s, 1H), 7.29 (d, J = 8.4 Hz, 2H), 7.42 (d, J = 8.4 Hz, 2H). ESMS: *m*/*z* 305.1 $(M + Na)^+$.

(c) *N*-*tert*-Butoxycarbonyl-*N*′-[2-(4-fluorophenyl)allyl]hydrazine (3c). The title compound was obtained as a white solid (1.9 g, 24%). mp: 83−84.5 °C. ^{1}H NMR ($CDCl_3$, 300 MHz): δ 1.48 (S, 9H), 3.87 (d, J = 4.5 Hz, 2H), 5.26 (d, J = 0.6 Hz, 1H), 5.43 (d, J = 0.6 Hz, 1H), 7.02 (t, J = 9 Hz, 2H), 7.47 (dd, J = 5.4, 7.8 Hz, 2H). ESMS: *m*/*z* 289.1 $(M+Na)^+$.

General Procedure for the Preparation of Compounds 5. A mixture of di-*tert*-butylhydrazodiformate (1.0 equiv) and NaH (1.0 equiv) in dimethylformade (DMF; 40.0 mL) was stirred at room temperature under N_2 for 20 min. To this solution was added a solution of substituted-α-bromomethylstyrene[16] (0.75 equiv) in DMF (5.0 mL). The resulting mixture was stirred at room temperature under N_2 for 7 h when TLC showed the reaction was completed. The reaction mixture was concentrated in vacuo. The residue was purified by flash column chromatography (silica gel, 0−5% EtOAc/hexane) to afford the desired product.

(a) *N*,*N*′-Di(*tert*-butoxycarbonyl)-*N*′-[2-(4-fluorophenyl)allyl]-hydrazine (5c). The title compound was obtained as a white solid (7.1 g, 89%). mp: 56−57.5 °C. ^{1}H NMR ($CDCl_3$, 300 MHz): δ 1.43 (s, 9H), 4.52 (br s, 2H), 5.14 (s, 1H), 5.42 (s, 1H), 6.95−7.02 (m, 2H), 7.29−7.51 (m, 2H). ESMS: *m*/*z* 389.1 $(M + Na)^+$.

(b) *N*,*N*′-Di(*tert*-butoxycarbonyl)-*N*′-[2-(2-methylphenyl)allyl]-hydrazine (5d). The title compound was obtained as a white solid (6.87 g, 76%). mp: 104−105 °C. ^{1}H NMR ($CDCl_3$, 300 MHz): δ 1.46 (s, 9H), 2.31 (s, 3H), 4.30 (br s, 2H), 5.04 (br s, 1H), 5.28 (d, J = 11.9 Hz, 1H), 6.98−7.19 (m, 4H). ESMS: *m*/*z* 385.1 $(M + Na)^+$.

General Procedure for the Preparation of Compounds 6. A mixture of **5c** (1.0 equiv) and NaH (1.6 equiv) in DMF (30 mL) was stirred at room temperature for 20 min. To this stirred solution were added alkyl halides (1.6 equiv). The resulting mixture was stirred at room temperature under N_2 overnight. The TLC showed the reaction was completed. The solvent was removed in vacuo. The residue was purified by flash column chromatography (silica gel, 0−5% EtOAc/hexane) to provide the desired product.

(a) *N*,*N*′-Di(*tert*-butoxycarbonyl)-*N*′-[2-(4-fluorophenyl)allyl]-*N*-methylhydrazine (6a). The title compound was obtained as a colorless oil (1.02 g, 98%). ^{1}H NMR ($CDCl_3$, 300 MHz): δ 1.40 (s, 9H), 1.42, 1.45 (two s, total 9H), 2.75 (s, 3H), 3.95−4.03 (m, 2H), 5.20 (s, 1H), 5.49 (s, 1H), 6.95−7.08 (m, 2H), 7.40−7.55(m, 2H). ESMS: *m*/*z* 403.1 $(M + Na)^+$.

(b) *N*,*N*′-Di(*tert*-butoxycarbonyl)-*N*′-[2-(4-fluorophenyl)allyl]-*N*-ethylhydrazine (6b). The title compound was obtained as a colorless oil (1.00 g, 93%). ^{1}H NMR ($CDCl_3$, 300 MHz): δ 0.92 (t, J = 7.2 Hz, 3H), 1.40 (s, 9H), 1.42, 1.44 (two s, total 9H), 3.06 (q, J = 7.2 Hz, 2H), 3.90−3.99 (m, 2H), 5.21 (S, 1H), 5.48 (s, 1H), 6.95−7.08 (m, 2H), 7.35−7.55 (m, 2H). ESMS: *m*/*z* 417.1 $(M + Na)^+$.

(c) *N*,*N*′-Di(*tert*-butoxycarbonyl)-*N*′-[2-(4-fluorophenyl)allyl]-*N*-isopropylhydrazine (6c). The title compound was obtained as a colorless oil (1.00 g, 90%). ^{1}H NMR ($CDCl_3$, 300 MHz): δ 1.02 (d, J = 6.9 Hz, 3H), 1.13 (d, J = 6.9 Hz, 3H), 1.39 (s, 9H), 1.45, 1.47 (two s, total 9H), 3.39−3.63 (m, 1H), 3.78−3.93 (m, 1H), 5.22 (s, 1H), 5.49 (s, 1H), 6.94−7.06 (m, 2H), 7.36−7.54 (m, 2H). ESMS: *m*/*z* 431.2 $(M + Na)^+$.

(d) *N*,*N*′-Di(*tert*-butoxycarbonyl)-*N*′-[2-(4-fluorophenyl)allyl]-*N*-benzylhydrazine (6d). The title compound was obtained as a colorless oil (0.87 g, 70%). ^{1}H NMR ($CDCl_3$, 300 MHz): δ 1.38 (s, 9H), 1.43, 1.47 (two s, total 9H), 4.08 (d, J = 15.0 Hz, 2H), 4.54 (d, J = 14.7 Hz, 1H), 4.80 (d, J = 14.7 Hz, 1H), 5.14 (s, 1H), 5.45 (s, 1H), 6.86−7.07 (m, 2H), 7.12−7.28 (m, 5H), 7.42−7.58 (m, 2H). ESMS: *m*/*z* 479.1 $(M + Na)^+$.

General Procedure for the Preparation of Compounds 8. A mixture of **3c** (1.0 equiv) and *N*,*N*-diisopropylethylamine (2.0 equiv) in DMF (10 mL) was stirred at room temperature for 20 min. To this solution were added alkyl halides (2.0 equiv). The resulting mixture was stirred at room temperature overnight. The TLC showed the reaction was completed. The solvent was removed in vacuo. The residue was purified by flash column chromatography (silica gel, 5% EtOAc/hexane) to provide the product.

(a) *N*-*tert*-Butoxycarbonyl-*N*′-[2-(4-fluorophenyl)allyl]-*N*′-methylhydrazine (8a). The title compound was obtained as a white solid (0.62 g, 98%). mp: 95−96 °C. ^{1}H NMR ($CDCl_3$, 300 MHz): δ 1.42 (s, 9H), 2.61 (s, 3H), 3.73 (br s, 2H), 5.21 (s, 1H), 5.42 (s, 1H), 6.95−7.08 (m, 2H), 7.46−7.59 (m, 2H). ESMS: *m*/*z* 303.1 $(M + Na)^+$.

(b) *N*-*tert*-Butoxycarbonyl-*N*′-[2-(4-fluorophenyl)allyl]-*N*′-ethylhydrazine (8b). The title compound was obtained as a white solid (0.23 g, 42%). mp: 54−55 °C. ^{1}H NMR ($CDCl_3$, 300 MHz): δ 1.06 (t, J = 4.3 Hz, 3H), 1.41 (s, 9H), 2.86 (br s, 2H), 3.81 (br s, 2H), 5.24 (br s, 1H), 5.43 (br s 1H), 7.01 (t, J = 5.3 Hz, 2H), 7.55 (br s, 2H). ESMS: *m*/*z* 317.1 $(M + Na)^+$.

(c) *N*-*tert*-Butoxycarbonyl-*N*′-[2-(4-fluorophenyl)allyl]-*N*′-isopropylhydrazine (8c). The title compound was obtained as a white semisolid (0.38 g, 66%). ^{1}H NMR ($CDCl_3$, 300 MHz): δ 1.05 (d, J = 3.3 Hz, 6H), 1.40 (s, 9H), 3.21 (br s, 1H), 3.73 (br s, 2H), 5.28 (br s, 1H), 5.42 (br s, 1H), 7.01 (t, J = 5.2 Hz, 2H), 7.58 (br s, 2H). ESMS: m/z 331.1 $(M + Na)^+$.

(d) *N*-*tert*-Butoxycarbonyl-*N*′-[2-(4-fluorophenyl)allyl]-*N*′-benzylhydrazine (8d). The title compound was obtained as a white semisolid (0.40 g, 60%). ^{1}H NMR ($CDCl_3$, 300 MHz): δ 1.38 (s, 9H), 3.96 (br s, 2H), 4.10 (br s, 2H), 5.28 (br s, 1H), 5.45 (br s, 2H), 7.00 (t, J = 5.2 Hz, 2H), 7.19−7.22 (m, 5H), 7.48 (br s, 2H). ESMS: m/z 379.1 $(M + Na)^+$.

***N*,*N*′-Di(*tert*-butoxycarbonyl)-*N*′-[2-(4-chlorophenyl)allyl]-*N*,*N*′-dimethylhydrazine (10).** A mixture of **3b** (0.42 g, 1.49 mmol) and NaH (0.11 g, 4.58 mmol) in DMF (10 mL) was stirred at room temperature for 20 min. To this stirred solution was added MeI (0.64 g, 4.51 mmol). The resulting reaction mixture was stirring under N_2 at room temperature overnight. The TLC showed the reaction was completed. The solvent was removed in vacuo. The residue was purified by flash column chromatography (silica gel, 5% EtOAc/Hexane) to give a colorless oil (0.29 g, 63%). ^{1}H NMR ($CDCl_3$, 300 MHz): δ 1.43 (s, 9H), 2.59 (s, 3H), 2.73 (s, 3H), 3.73 (br s, 2H), 5.22 (s, 1H), 5.43 (s, 1H), 7.33 (d, J = 8.7 Hz, 2H), 7.41 (d, J = 8.7 Hz, 2H). ESMS: m/z 333.1 $(M + Na)^+$.

General Procedure for the Preparation of Compounds 4, 7, 9, and 11. To a solution of Boc protected hydrazine compounds (1.0 equiv.) in anhydrous MeOH (3.0 mL) was added a solution of HCl in ether (5.0 equiv.). The resulting mixture was stirred under N_2 at room temperature and monitored by TLC. When TLC showed that the reaction was completed, it was concentrated in vacuo. The residue was dissolved in H_2O (20 mL). The resulting aqueous solution was washed with ether (2 × 10 mL) and then was basified to pH 10 by adding 1.0 N NaOH solution. The resulting basic solution was saturated with solid NaCl and extracted with ether (3 × 30 mL). The combined organic layers were dried ($MgSO_4$), filtered and concentrated in vacuo. The residue was dissolved in ether (5.0 mL). To this solution was added a solution of HCl in ether (5 equiv.). The solid formed was collected by filtration, washed with ether, and then dried in vacuo to give the final compounds as hydrochloride salts.

(a) *N*′-(2-Phenylallyl)hydrazine Hydrochloride (4a). The title compound was obtained as a white solid (0.66 g, 90%). mp: 153−154.5 °C. ^{1}H NMR (D_2O, 300 MHz): δ 4.05 (s, 2H), 5.40 (s, 1H), 5.60 (s, 1H), 7.25−7.42 (m, 5H). ESMS: m/z 149 $(M + H)^+$. Anal. ($C_9H_{13}ClN_2$) C, H, N.

(b) *N*′-[2-(4-Chlorophenyl)allyl]hydrazine Hydrochloride (4b). The title compound was obtained as a white solid (0.60 g, 100%). mp: 124−126 °C. ^{1}H NMR (D_2O, 300 MHz): δ 4.06 (s, 2H), 5.43 (s, 1H), 5.65 (s, 1H), 7.35 (d, J = 9.0 Hz, 2H), 7.40 (d, J = 9.0 Hz, 2H). ESMS: m/z 183 $(M + H)^+$. Anal. ($C_9H_{12}Cl_2N_2$) C, H, N.

(c) *N*′-[2-(4-Fluorophenyl)allyl]hydrazine Hydrochloride (4c). The title compound was obtained as a off-white solid (0.55 g, 90%). mp: 149−150 °C. ^{1}H NMR (D_2O, 300 MHz): δ 4.16 (s, 2H), 5.49 (s, 1H), 5.70 (s, 1H), 7.07 (t, J = 8.7 Hz, 2H), 7.42 (dd, J = 5.4, 8.7 Hz, 2H). ESMS: m/z 167 $(M + H)^+$. Anal. ($C_9H_{12}ClFN_2$) C, H, N.

(d) *N*′-[2-(2-Methylphenyl)allyl]hydrazine Hydrochloride (4d). The title compound was obtained as a white powder (0.56 g, 95%). mp: 107−108.5 °C. ^{1}H NMR (D_2O, 300 MHz): δ 2.30 (s, 3H), 4.02 (s, 2H), 5.35 (s, 1H), 5.65 (s, 1H), 7.16−7.28 (m, 2H), 7.28−7.34 (m, 2H). ESMS: m/z 163 $(M + H)^+$. Anal. ($C_{10}H_{15}ClN_2$) C, H, N.

(e) *N*′-[2-(4-Fluorophenyl)allyl]-*N*-methylhydrazine Hydrochloride (7a). The title compound was obtained as a white solid (0.52 g, 90%). mp: 128−129 °C. ^{1}H NMR (D_2O, 300 MHz): δ 2.66 (s, 3H), 3.95 (s, 2H), 5.29 (s, 1H), 5.50 (s, 1H), 7.03 (t, J = 9.0 Hz, 2H), 7.42 (t, J = 9.0 Hz, 2H). ESMS: m/z 181 $(M + H)^+$. Anal. ($C_{10}H_{14}ClFN_2$) C, H, N.

(f) *N*′-[2-(4-Fluorophenyl)allyl]-*N*-ethylhydrazine Hydrochloride (7b). The title compound was obtained as a white solid (0.44 g, 90%). mp: 117−118 °C. ^{1}H NMR (D_2O, 300 MHz): δ 1.10 (t, J = 7.2 Hz, 3H), 3.04 (q, J = 6.9 Hz, 2H), 3.93 (s, 2H), 5.30 (s, 1H), 5.50 (s, 1H), 7.04 (t, J = 9.0 Hz, 2H), 7.42 (t, J = 9.0 Hz, 2H). ESMS: m/z 195 $(M + H)^+$. Anal. ($C_{11}H_{16}ClFN_2$) C, H, N.

(g) *N*′-[2-(4-Fluorophenyl)allyl]-*N*-isopropylhydrazine Hydrochloride (7c). The title compound was obtained as a white solid (0.42 g, 82%). mp: 140−141 °C. ^{1}H NMR (D_2O, 300 MHz): δ 1.12 (d, J = 6.6 Hz, 6H), 3.25−3.44 (m, 1H), 3.92 (s, 2H), 5.29 (s, 1H), 5.50 (s, 1H), 7.04 (t, J = 8.7 Hz, 2H), 7.40−7.47 (m, 2H). ESMS: m/z 209 $(M + H)^+$. Anal. ($C_{12}H_{18}ClFN_2$) C, H, N.

(h) *N*′-[2-(4-Fluorophenyl)allyl]-*N*-benzylhydrazine Hydrochloride (7d). The title compound was obtained as a light yellow solid (0.44 g, 90%). mp: 149−150 °C. ^{1}H NMR (D_2O, 300 MHz): δ 4.01 (s, 2H), 4.16 (s, 2H), 5.32 (s, 1H), 5.53 (s, 1H), 7.03 (t, J = 8.7 Hz, 2H), 7.28−7.60 (m, 2H). ESMS: m/z 257 $(M + H)^+$. Anal. ($C_{16}H_{18}ClFN_2$) C, H, N.

(i) *N*′-[2-(4-Fluorophenyl)allyl]-*N*′-methylhydrazine Hydrochloride (9a). The title compound was obtained as a white solid (0.40 g, 95%). mp: 138−140 °C. ^{1}H NMR (D_2O, 500 MHz): δ 2.72 (s, 3H), 4.05 (s, 2H), 5.43 (s, 1H), 5.62 (s, 1H), 7.06 (t, J = 8.7 Hz, 2H), 7.39−7.48 (m, 2H). ESMS: m/z 181 $(M + H)^+$. Anal. ($C_{10}H_{14}ClFN_2$) C, H, N.

(j) *N*′-[2-(4-Fluorophenyl)allyl]-*N*′-ethylhydrazine Hydrochloride (9b). The title compound was obtained as a white solid (0.14 g, 90%). mp: 118−119 °C. ^{1}H NMR (D_2O, 500 MHz): δ 1.27 (t, J = 7.3 Hz, 3H), 3.24 (br s, 2H), 4.28 (br s, 2H), 5.61 (s, 1H), 5.78 (s, 1H), 7.18 (t, J = 8.7 Hz, 2H), 7.54 (dd, J = 5.3, 8.7 Hz, 2H). ESMS: m/z 195 $(M + H)^+$. Anal. ($C_{11}H_{16}ClFN_2$) C, H, N.

(k) *N*′-[2-(4-Fluorophenyl)allyl]-*N*′-isopropylhydrazine Hydrochloride (9c). The title compound was obtained as a white solid (0.22 g, 85%). mp: 146−147 °C. ^{1}H NMR (D_2O, 500 MHz): δ 1.31 (d, J = 6.7 Hz, 3H), 3.56−3.71 (m, 1H), 4.10−4.30 (m, 2H), 5.63 (s, 1H), 5.78 (s, 1H), 7.19 (t, J = 8.7 Hz, 2H), 7.54 (d, J = 5.3, 8.7 Hz, 2H). ESMS: m/z 209 $(M + H)^+$. Anal. ($C_{12}H_{18}ClFN_2$) C, H, N.

(l) *N*′-[2-(4-Fluorophenyl)allyl]-*N*′-benzylhydrazine Hydrochloride (9d). The title compound was obtained as a white solid (0.25 g, 90%). mp: 170−171 °C. ^{1}H NMR (D_2O, 500 MHz): δ 4.06 (s, 2H), 4.17 (s, 2H), 5.51 (s, 1H), 5.70 (s, 1H), 7.12 (t, J = 8.7 Hz, 2H), 7.28−7.37 (m, 2H), 7.38−7.50 (m, 5H). ESMS: m/z 257 $(M + H)^+$. Anal. ($C_{16}H_{18}ClFN_2$) C, H, N.

(m) *N*′-[2-(4-Chlorophenyl)allyl]-*N*,*N*′-dimethylhydrazine Hydrochloride (11). The title compound was obtained as a white solid (0.17 g, 74%). mp: 108−110 °C. ^{1}H NMR (D_2O, 300 MHz): δ 2.58 (s, 3H), 2.69 (s, 3H), 3.93 (s, 2H), 5.42 (s, 1H), 5.60 (s, 1H). HRMS (MALDI−FTMS). Calcd for $C_{11}H_{15}ClN_2H$: 211.0995. Found: 211.0995.

***N*′-[(*E*)−(2-Phenyl-3-fluoroallyl)]-*N*′-*tert*-butoxycarbonylaminophthalimide (14).** To a cooled solution of (*E*)-2-phenyl-3-fluoroallyl alcohol **12** [17a] (1.1 g, 7.47 mmol), PPh_3 (2.94 g, 11.22 mmol), and *N*-*tert*-butoxycarbonylaminophthalimide **13** [17b] (1.95 g, 7.47 mmol) in tetrahydrofuran (THF; 120 mL) was added dropwise a solution of diethyl azodicarboxylate (DEAD) (1.8 mL, 11.09 mmol) in THF (5.0 mL). The resulting mixture was stirred under N_2 at room temperature overnight and then concentrated in vacuo. The residue was purified by flash column chromatography (silica gel, 10% EtOAc/haxane) to give a colorless oil (1.3 g, 44%). ^{1}H NMR ($CDCl_3$, 300 MHz): δ 1.30, 1.44 (two s, total 9H), 4.55, 4.63 (two s, 2H), 6.81 (two d, J = 81.0 Hz, 1H), 7.23−7.45 (m, 5H), 7.71−7.95 (m, 4H). ESMS: m/z 419.1 $(M + Na)^+$.

***N*′-[(*E*)−(2-Phenyl-3-fluoroallyl)]hydrazine Hydrochloride (15).** A mixture of **14** (1.3 g, 3.28 mmol), NH_2NHMe (0.26 mL, 4.72 mmol) in THF (50 mL) was stirred under N_2 at room temperature for 24 h and then concentrated in vacuo. The residue was diluted with EtOAc. The solid formed was filtered and washed with EtOAc. The combined filtrate was concentrated in vacuo to give a semisolid (0.98 g). It was used directly in the next step without any further purification. It was dissolved in MeOH (5.0 mL). To this solution was added HCl solution in 1,4-dioxane (4.0 M, 4.0 mL, 16 mmol). The resulting mixture was stirred under N_2 at room temperature overnight and then concentrated in vacuo. The residue was diluted with ether (30 mL) and filtered. The solid was washed with ether

(3 × 30 mL) and EtOAc (3 × 30 mL) and then dried in vacuo to give a white solid (0.35 g, 53%). mp: 139−141 °C. ^{1}H NMR (D_2O, 300 MHz): δ 3.89 (s, 2H), 6.96 (d, J = 81.0 Hz, 1H), 7.25−7.46 (m, 5H). ESMS: m/z 167 $(M + H)^+$. Anal. ($C_9H_{12}ClFN_2$) C, H, N.

Preparation of Rat Lung Homogenates. Freshly excised rat lungs were cut into small pieces, and then washed thoroughly with PBS. The washed tissue was then homogenized at 1:20 (w/v) in 10 mM solution of potassium phosphate buffer (pH 7.8). The homogenate was then centrifuged at 10000*g* for 10 min at 4 °C. The supernatant was collected and kept frozen until ready to use.

Radiochemical assays: SSAO activity was measured as described by Fowler.[18] Briefly, SSAO activity in 100 μL of lung homogenate was determined radiochemically using 20 μM benzylamine-^{14}C as substrate and a determined amount of inhibitor. The reaction was carried out at 37 °C in a final volume of 400 μL of 100 mM potassium phosphate buffer (pH 7.2) and stopped with 100 μL of 2.0 M citric acid. Radioactively labeled products were extracted into toluene/ethyl acetate (1:1, v/v) containing 0.6% (w/v) 2,5-diphenyloxazole (PPO) before liquid scintillation counting. All experiments were performed in the presence of clorgyline and pargyline for total inhibition of MAO-A and MAO-B activities in the tissue homogenate. Inhibition was calculated as percent inhibition compared to control after correcting for background counts, and IC_{50} values were calculated from a dose−response curve using GraphPad Prism software (version 3.03; San Diego, CA).

Enzyme Kinetic Study. Kinetic parameters were determined using the radiochemical assay as described above. Briefly, rat lung homogenates (25 μL) were incubated at 37 °C for 1 min with various concentrations of benzylamine-^{14}C (0.1−10 μM) in the absence or presence of compound **4a** (1−5 nM), then was kept in ice, and quenched by adding 2 M citric acid solution (100 μL). Following the workup procedures described above for the radiochemical assay, the V_{max} for each reaction was calculated using GraphPad Prism software.

Dialysis Experiments. To test whether reversible or irreversible inhibition was produced by compound **4a**, rat lung homogenates were preincubated for 30 min with appropriate concentrations of compound **4a** to bring about complete or virtually complete inhibition of SSAO activity. These samples were dialyzed at 4 °C in an attempt to restore enzyme activity. Dialyzed samples including uninhibited controls were assayed and compared with corresponding nondialyzed samples otherwise treated identically.

Time-Dependent Inhibition Experiments. These experiments were carried out by using the method described by Kitz and Wilson.[22] Briefly, mixtures containing rat lung homogenates (25 μL) and appropriate amount of **4a** to give inhibitor concentration from 10 to 100 nM were set up in ice-cold vessels and then preincubated for various periods at 37 °C. After the appropriate times, a 1:100 dilution was made for each mixture with ice-cold 0.2 M potassium phosphate buffer, pH 7.6. SSAO activity after dilution was assayed by incubation of diluted sample (390 μL) with 400 nM benzylamine-^{14}C (10 μL) at 37 °C for 30 min.

In Vivo Acute EAE Animal Study. To induce EAE on 7−8 week old C57BL/6 female mice, MOG_{35-55} in CFA containing 3.0 mg/mL *Mycobacterium tuberculosis* H37Ra (Difco, Detroit, MI) was injected at a dose of 300 μg over two sites at the back of the mice. Pertussis toxin (500 ng) was given intraperitoneally (ip) on days 0 and 2 postimmunization. Compound **4a** (20 (mg/kg)/dose, 1 dose/day), Methotrexate (MTX) in saline (3 mg/kg, once a day on M, W, F) and buffer were administered ip for 25 days starting from day 1. Animals were monitored for body weight (M, W, F from day 1), signs of paralysis, and death (M, W, and F from day 10). EAE clinical severity was scored according to a 0−5 scale system.

Statistical Analysis. Statistical analysis was performed using a repeated measure analysis to assess the treatment effect, and results were considered to be significant if $p < 0.05$.

Acknowledgment. We thank Dr. Tenshang Joh, Dr. Shaw-Ling Wang, and Mr. Dan Konkler for performing statistical analyses on EAE studies.

Supporting Information Available: Results from elemental analysis (pdf). This material is available free of charge via the Internet at http://pubs.acs.org.

References

(1) Holt, A.; Alton, G.; Scaman, C. H.; Loppnow, G. R.; Szpacenko, A.; Svendsen, I.; Palcic, M. M. Identification of the Quinone Cofactor in Mammalian Semicarbazide-Sensitive Amine Oxidase. *Biochemistry* **1998**, *37*, 4946−4957.

(2) Buffoni F.; Ignesti G. The Copper-Containing Amine Oxidases: Biochemical Aspects and Functional Role. *Mol. Genet. Metab*. **2000**, *71*, 559−564, and references cited within.

(3) Lyles, G. A. Mammalian Plasma and Tissue-Bound Semicarbazide-Sensitive Amine Oxidase: Biochemical, Pharmacological and Toxicological Aspects. *Int. J. Biochem. Cell Biol*. **1996**, *28*, 259−274.

(4) Stolen, C. M.; Yegutkin, G. G.; Kurkijarvi, R.; Bono, P.; Alitalo, K.; Jalkanen, S. Origins of Serum Semicarbazide-Sensitive Amine Oxidase. *Circ. Res*. **2004**, *95*, 50−57.

(5) (a) Zhang, X.; McIntire, W. S. Cloning and Sequencing of a Copper-Containing, Topa Quinone-Containing Monoamine Oxidase from Human Placenta. *Gene* **1996**, *179*, 279−286. (b) Smith, D. J.; Salmi, M.; Bono, P.; Hellman, J.; Leu, T.; Jalkanen, S. Cloning of Vascular Adhesion Protein 1 Reveals a Novel Multifunctional Adhesion Molecule. *J. Exp. Med*. **1998**, *188*, 17−27.

(6) (a). Salmi, M.; Jalkanen, S. VAP-1: An Adhesion and an Enzyme. *Trends Immunol*. **2001**, *22*, 211−216. (b). Moldes, M.; Fève, B.; Pairault, J. Molecular Cloning of a Major mRNA Species in Murine 3T3 Adipocyte Lineage. Differentiation-Dependent Expression, Regulation, and Identification as Semicarbazide-Sensitive Amine Oxidase. *J. Biol. Chem*. **1999**, *274*, 9515−9523.

(7) Jaakkola, K.; Nikula, T.; Holopainen, R.; Vahasilta, T.; Matikainen, M. T.; Laukkanen, M. L.; Huupponen, R.; Halkola, L.; Nieminen, L.; Hiltunen, J.; Parviainen, S.; Clark, M. R.; Knuuti, J.; Savunen, T.; Kaapa, P.; Viopio-Pulkki, L. M.; Jalkanen, S. In Vivo Detection of Vascular Adhesion Protein-1 in Experimental Inflammation. *Am. J. Pathol*. **2000**, *157*, 463−471.

(8) Salmi, M.; Yegutkin, G. G.; Lehvonen, R.; Koskinen, K.; Salminen, T.; Jalkanen, S. A Cell Surface Amine Oxidase Directly Controls Lymphocyte Migration. *Immunity* **2001**, *14*, 265−276.

(9) O'Sullivan, J.; Unzeta, M.; Healy, J.; O'Sullivan, M. I.; Davey, G.; Tipton, K. F. Semicarbazide-Sensitive Amine Oxidases: Enzymes with Quite a Lot To Do. *Neurotoxicology* **2004**, *25*, 303−315.

(10) Yu, P. Involvement of Cerebrovascular Semicarbazide-Sensitive Amine Oxidase in the Pathogenesis of Alzheimer's Disease and Vascular Dementia. *Med. Hypotheses* **2001**, *57*, 175−179.

(11) Stolen, C. M.; Madanat, R.; Marti, L.; Kari, S.; Yegutkin, G. G.; Sariola, H.; Zorzano, A.; Jalkanen, S. Semicarbazide Sensitive Amine Oxidase Overexpression Has Dual Consequences: Insulin Mimicry and Diabetes-like Complications. *FASEB J*. **2004**, *18*, 702−704.

(12) Stolen, C. M.; Marttila-Ichihara, F.; Koskinen, K.; Yegutkin, G. G.; Turja, R.; Bono, P.; Skurnik, M.; Hanninen, A.; Jalkanen, S.; Salmi, M. Absence of the Endothelial Oxidase AOC3 Leads to Abnormal Leukocyte Traffic *in Vivo*. *Immunity* **2005**, *22*, 105−115.

(13) Mátyus, P.; Dajka-Halász, B.; Földi, Á.; Haider, N.; Barlocco, D.; Magyar, K. Semicarbazide-Sensitive Amine Oxidase: Current Status and Perspectives. *Curr. Med. Chem.* **2004**, *11*, 1285−1298, and references cited therein.

(14) Andree, T. H.; Clarke, D. E. Characteristics and Specificity of Phenelzine and Benserazide as Inhibitors of Benzylamine Oxidase and Monoamine Oxidase. *Biochem. Pharmacol.* **1982**, *31*, 825−830.

(15) Lyles, G. A.; Marshall, C. M. S.; McDonald, I.; Bey, P.; Palfreyman, M. G. Inhibition of Rat Aorta Semicarbazide-Sensitive Amine Oxidase By 2-Phenyl-3-haloallylamines and Related Compounds. *Biochem. Pharmacol*. **1987**, *36*, 2847−2853.

(16) (a). Reed, S., Jr. Allylic Halogenation of α-Methylstyrene. Preparation of α-Chloromethylstyrene. *J. Org. Chem*. **1962**, *27*, 1921. (b). Yamanaka, M.; Arisawa, M.; Nishida, A.; Nakagawa, M. An Intriguing Effect of $Yb(Otf)_3$−TMSCl in the Halogenation of 1,1-Disubstituted Alkenes By NXS: Selective Synthesis of Allyl Halides. *Tetrahedron Lett*. **2002**, *43*, 2403−2406.

(17) (a) McDonald, I.; Lacoste, J.; Bey, P.; Palfreyman, M.; Zreika, M. Enzyme-Activated Irreversible Inhibitor of Monoamine Oxidase: Phenylallylamine Structure−Activity Relationships. *J. Med. Chem*. **1985**, *28*, 186−193. (b) Brosse, N.; Pinto, M.-F.; Jamart-Grégoire, B. New Synthesis of 1,1-Substituted Hydrazines by Alkylation of N-Acyl or N-Alkyloxycarbonylaminophthalimide Using the Mitsunobu Protocol. *J. Org. Chem*. **2000**, *65*, 4370−4374.

(18) Fowler, C. J.; Tipton, K. F. Concentration Dependence of the Oxidation of Tyramine by the Two Forms of Rat Liver Mitochondrial Monoamine Oxidase. *Biochem. Pharmacol*. **1981**, *30*, 3329−3332.
(19) Boomsma, F.; Dijk, J. v.; Bhaggoe, U. M.; Bouhuizen, A. M. B.; Meiracker, A. v. d. Variation in Semicarbazide-Sensitive Amine Oxidase Activity in Plasma and Tissues of Mammals. *Comp Biochem. Physiol., Part C: Pharmacol., Toxicol. Endocrinol*. **2000**, *126*, 69−78.
(20) Holt, A.; Sharman, D. F.; Baker, G. B.; Palcic, M. M. A Continuous Spectophotometric Assay for Monoamine Oxidase and Related Enzymes in Tissue Homogenates. *Anal. Biochem.* **1997**, *244*, 3384−3392.
(21) La Jolla Pharmaceutical Co. Unpublished results.
(22) Kitz, R.; Wilson I. B. Ester of Methanesulfonic Acid as Irreversible Inhibitors of Acetylcholinesterase. *J. Biol. Chem*. **1962**, *237*, 3245−3249.
(23) These studies were conducted by Cerep (Seattle, WA).
(24) (a) Xu, H.-L.; Salter-Cid, L.; Linnik, M. D.; Wang, E.; Paisansathan, O.; Pelligrino, D. A. Vascular Adhesion Protein-1 Plays an Important Role in Post-Ischemic Inflammation and Neutophathology in Diabetic, Estrogen-Treated Ovariectomized Female Rats Subjected to Transient Forebrain Ischemia. *J. Pharmacol. Exp. Ther*. **2005** (Dec 8) [epub ahead of print]. (b). Salter-Cid, L.; Wang, E.; O'Rourke, A.; Miller, A.; Gao, H.; Huang, L.; Garcia, A.; Linnik, M. D. Anti-Inflammatory Effects of a Small Molecule Antagonist of SSAO/VAP-1. *J. Pharmacol. Exp. Ther.* **2005**, *315*, 553−562.
(25) Hafler, D. A. Multiple Sclerosis. *J. Clin. Invest*. **2004**, *113*, 788−94.
(26) Koskinen, K.; Vainio, P. J.; Smith, D. J.; Pihlavisto, M.; Yla-Herttuala, S.; Jalkanen, S.; Salmi, M. Granulocyte Transmigration through the Endothelium Is Regulated by the Oxidase Activity of Vascular Adhesion Protein-1 (VAP-1). *Blood* **2004**, *103*, 3388−3395.

JM050538L